Characteristics of Double Exponentially Tapered Slot Antenna (DETSA) Conformed in the Longitudinal Direction Around a Cylinder

George E. Ponchak, *Senior Member, IEEE*, Jennifer L. Jordan, and Christine T. Chevalier, *Student Member, IEEE*

***Abstract*—The characteristics of a double exponentially tapered slot antenna (DETSA) as a function of the radius that the DETSA is conformed to in the longitudinal direction is presented. It is shown through measurements and simulations that the radiation pattern of the conformed antenna rotates in the direction through which the antenna is curved, and that diffraction affects the radiation pattern if the radius of curvature is too small or the frequency too high. The gain of the antenna degrades by only 1 dB if the radius of curvature is large and more than 2 dB for smaller radii. The main effect due to curving the antenna is an increased cross polarization in the E-plane.**

***Index Terms*—Conformal antenna, double exponentially tapered slot antenna (DETSA), slot-line antenna.**

I. Introduction

THE family of tapered slot antennas (TSAs) are useful because they have a wide 10–dB return loss bandwidth, are easy to fabricate on a variety of substrates, and have good radiation pattern characteristics with moderate gain of approximately 8 dBi [1]. The first implementation of a TSA was a stripline fed antenna formed in the ground planes [2], the first printed slot antenna was an exponentially tapered slot, the Vivaldi Antenna [3], and a double exponentially tapered slot antenna (DETSA) has been introduced [4]. Various forms of TSAs have been summarized [5], and almost all past research has been on flat antennas. However, it has also been noted that because they may be printed on thin, soft substrates such as liquid crystal polymer (LCP), they may be conformal [1], [6], and [7], which is required for mounting antennas on automobiles, aircraft wings, and wearable wireless networks.

In [6], a brief summary of an experiment about wrapping a TSA around a foam cylinder with the discontinuity in the transverse and longitudinal direction is presented. Only the effect on gain is described, with no discussion of the radiation pattern. A DETSA designed for ultrawide band (UWB) applications conformed over a gently rounded foam shape in the longitudinal direction is described in [7]. It was shown that, for the single case presented, the main beam is skewed toward the direction of curvature.

Manuscript received September 1, 2006; revised December 12, 2006.

G. E. Ponchak and J. L. Jordan are with NASA Glenn Research Center, Cleveland, OH 44135 USA (george.ponchak@ieee.org; Jennifer.Jordan@grc.nasa.gov).

C. T. Chevalier is with Analex Corp at NASA Glenn Research Center, Cleveland, OH 44135 USA (Christine.Chevalier@grc.nasa.gov).

Digital Object Identifier 10.1109/LAWP.2007.890764

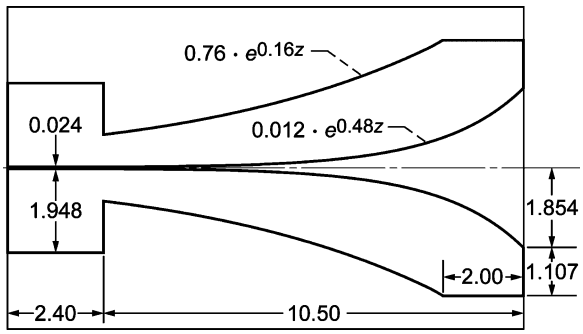

Fig. 1. Schematic of DETSA with dimensions in cm.

TABLE I
DIMENSIONS OF DETSA RADII OF CURVATURE

Radius (cm)	Radius (λ_0 at 6 GHz)	Angle DETSA wraps around circle (degree)
4.46	0.89	135
6.685	1.38	90
13.37	2.68	45
26.74	5.35	22.5

In this letter, experimental and simulated characteristics of a DETSA conformed in the longitudinal direction around a cylindrical, foam structure is presented. The gain, 3–dB beamwidth, cross-polarization level, and beam direction are presented for different cylinder radii.

II. DETSA Description

A DETSA was fabricated with 18-μm- thick copper on a 200-μm-thick LCP substrate, which has a dielectric constant ε_r of 3.1 and a loss tangent of 0.003 [8]. The DETSA was optimized to operate over the frequency range of 4 to 10 GHz when flat. Fig. 1 shows a schematic of the DETSA with all dimensions and the equations for the exponential tapers. The slotline width at the start of the taper is 240 μm.

The radii of curvature are given in Table I. Note that, throughout the letter, the data are presented as a function of the angle that the DETSA wraps around a cylinder, with the uniform section of slotline held flat. For example, for the cylinder with a radius of 6.685 cm, the DETSA wraps one quarter, or 90°, around the cylinder. Fig. 2 shows a drawing of the curved DETSA wrapped 90° around a cylinder.

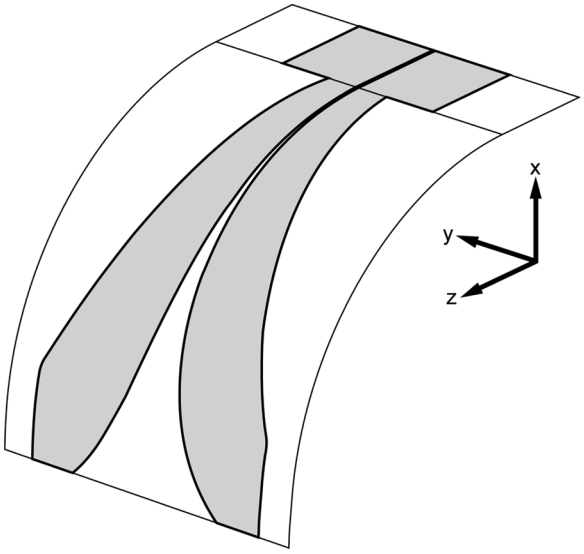

Fig. 2. Schematic of DETSA wrapped 90° around cylindrical structure.

III. Return Loss and Radiation Pattern Measurement Technique

The DETSA was held in a cylindrical shape by placing it between two pieces of Styrofoam ($\varepsilon_r = 1.03$). The Styrofoam is cut on a band saw, which introduces small variations (errors) to the shape. The beginning of the taper is placed where the Styrofoam starts to curve.

To feed the DETSA, the outer conductor of a semirigid coaxial waveguide is soldered onto one side of the slotline perpendicular to the slot at the edge of the board and the center conductor is extended to and soldered to the opposite side of the slotline [9]. Although the impedance match was not optimum, simulations and measurements showed that symmetric currents are established on the slotline, which is critical for radiation pattern characterization.

Reflection coefficient $|S_{11}|$ is measured on an HP 8510 Vector Network Analyzer. Far-field radiation E and H-plane measurements were made in a calibrated far-field antenna range from 3 to 9 GHz in 2 GHz increments. H-plane is measured in the xz plane in Fig. 2. E-plane is measured in the plane of the excitation feed (yz plane in Fig. 2), rather than in the direction of maximum H-plane radiation. As will be shown in Section V, taking E-plane measurements in the direction of maximum H-plane would require cutting 16 blocks of Styrofoam at specific angles. Thus, simulated E-plane patterns in the direction of the H-plane maximum are used.

IV. Simulation Method

The transient solver of the software package CST Microwave Studio [10] was used to simulate the DETSAs. The substrate material is of the type Normal with $\varepsilon_r = 3.1$. The antenna is patterned with the material perfect electric conductor (PEC). All materials are lossless. The Styrofoam used in the measurements was not modeled. The antenna shape is drawn using the polygon curve tool which is then extruded to add metal thickness. A discrete S-parameter port with an impedance of 50 Ω was used to excite the antenna. Automatic meshing of eight meshlines per wavelength was used. For the flat DETSA, this yields 555 540 mesh cells.

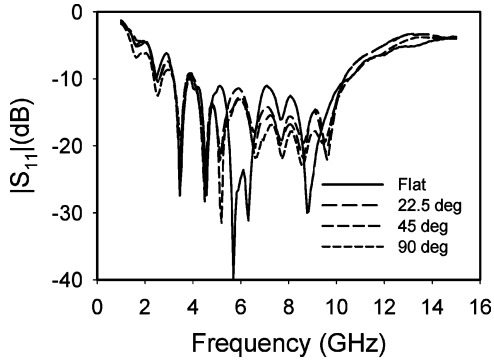

Fig. 3. Measured return loss of DETSA as a function of frequency and degree of curvature.

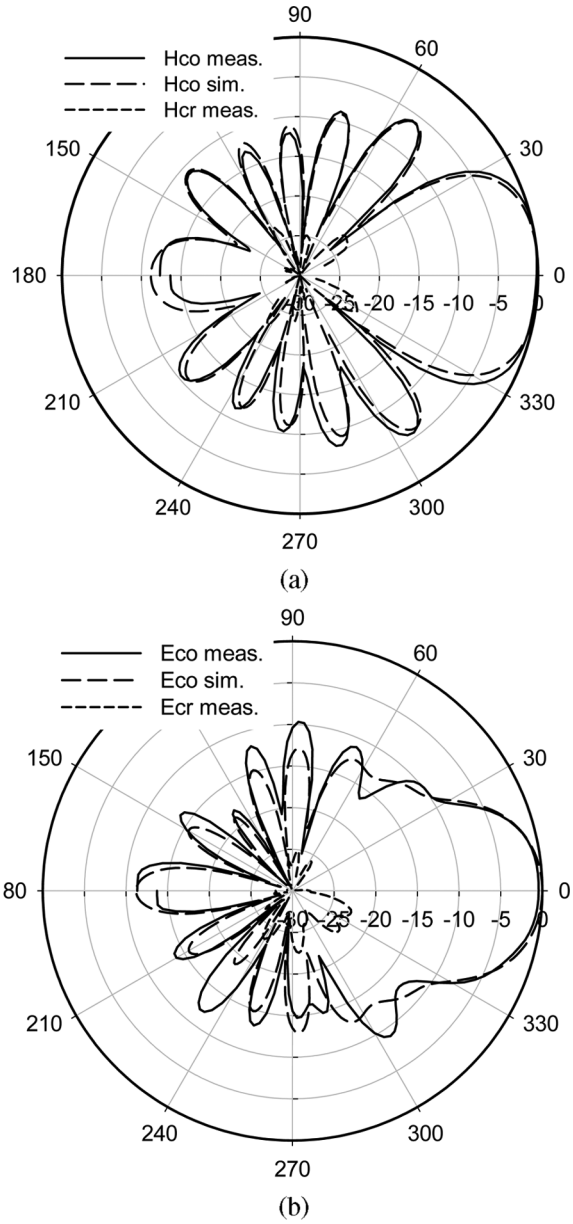

Fig. 4. Measured and simulated: (a) H-plane; and (b) E-plane radiation pattern for flat DETSA at 7 GHz.

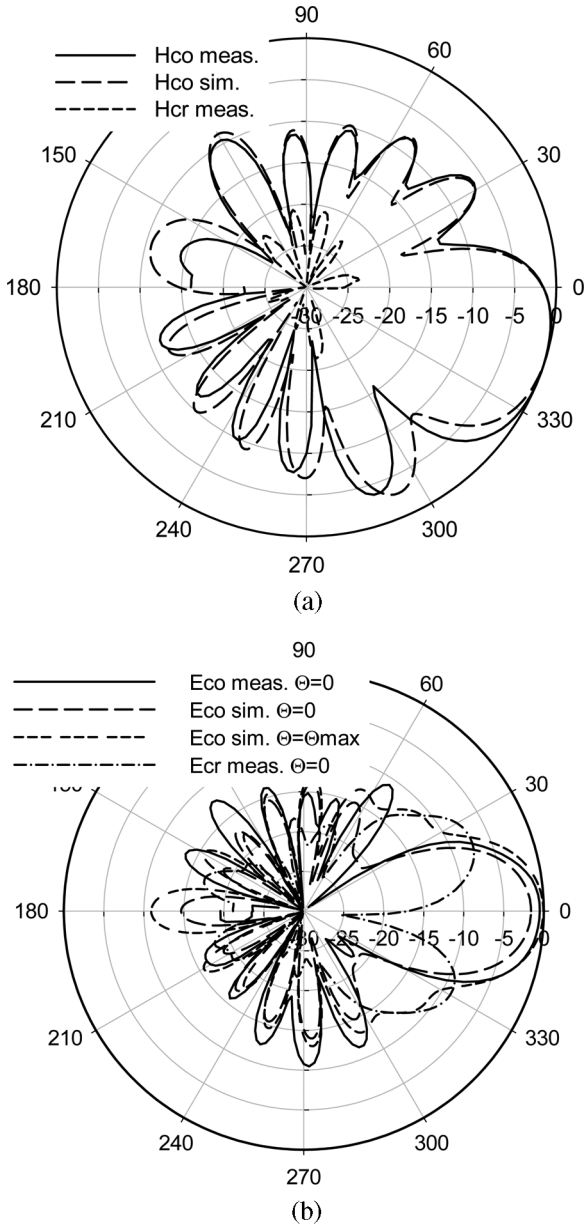

Fig. 5. Measured and simulated: (a) H-plane; and (b) E-plane radiation pattern for 45° DETSA at 7 GHz.

V. Results

The measured return loss is shown in Fig. 3 as a function of the degree of curvature. It is seen that the 10-dB bandwidth is from 3 to 10 GHz, regardless of the degree of curvature.

The radiation patterns for a flat DETSA and DETSAs conformed in the longitudinal direction 45° around a cylinder are shown in Figs. 4 and 5, respectively. The simulated cross-polarization values are not plotted for clarity, but they are summarized later. First, it is noted that there is excellent agreement between the measured and simulated radiation patterns. This permits the use of simulated data for E copolarization at the angle of maximum H copolarization where it is too difficult to configure the antennas for measurements. By comparing the flat DETSA H-plane pattern with the curved DETSA patterns,

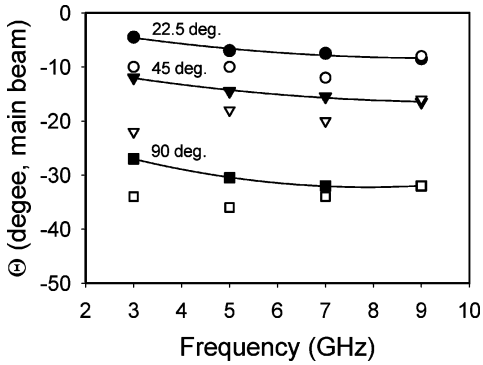

Fig. 6. Measured and simulated angle of maximum radiation in H-plane as a function of degree of curvature (solid symbols are simulated, open symbols are measured).

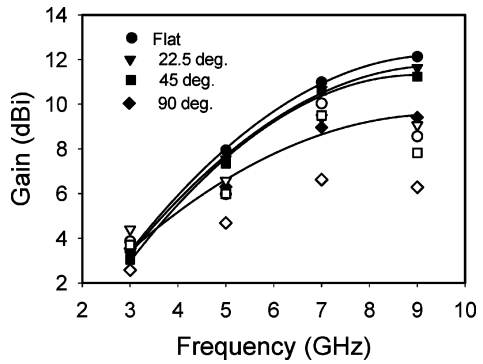

Fig. 7. Measured and simulated gain of DETSA as a function of degree of curvature (solid symbols are simulated, open symbols are measured).

it is seen that the number of nulls and lobes is the same. Furthermore, the location of the nulls and lobes relative to the main beam remains approximately equal. Therefore, the H-plane pattern appears to be a simple rotation towards the direction of curvature as the DETSA is conformed. As the radius of the cylinder decreases or the frequency increases, diffraction effects increase and the pattern below the antenna is affected. This is seen for the 45° curved antenna Fig. 5(a); note the larger sidelobes in the direction of 285°. It also affects the measured pattern characteristics at 90° as seen in Figs. 6–8. The H-plane radiation pattern of the 135° curved antenna, not shown, is severely affected by diffraction.

The angle that the H-plane pattern rotates, or the angle of the main beam, is presented in Fig. 6. The main beam is pointed in the direction that the antenna is curved. As an approximation, the main beam is pointed in the direction of the tangent of the DETSA at one third of its length from the feed line. A second observation is that the main beam points more towards the direction tangent to the end of the DETSA as the frequency increases. This agrees with the observation in [7].

The antenna gain is shown in Fig. 7. The measured gain has been corrected for the coaxial to slotline transition return loss, but not for any attenuation, while the simulated gain assumes a lossless antenna. As the frequency increases, the gain increases as expected for TSAs. The gain decreases by only 1 dB for DETSAs wrapped 45° or less around cylinder, but if the radius of curvature is greater, the gain decreases by an average of 2 dB across the frequency band. Interestingly, the gain for 22.5 and 45° curvature is almost the same.

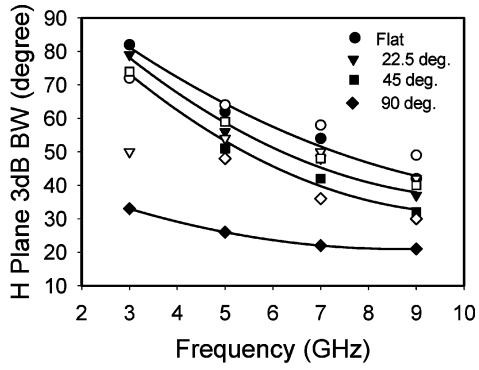

(a)

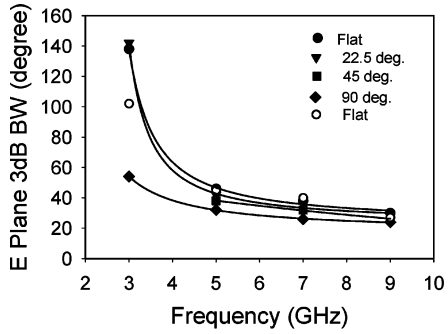

(b)

Fig. 8. Measured and simulated: (a) H-plane; and (b) E-plane 3-dB beamwidth (solid symbol are simulated, open symbol are measured).

The 3-dB beamwidth is plotted in Fig. 8. Again, the curved DETSA behaves similar to the flat DETSA, with 3-dB beamwidth decreasing with frequency. The beamwidth decreases as the antenna curvature increases, with the main beam in the H-plane decreasing by approximately 25°. The E-plane beamwidth is large at 3 GHz, but it is comparable to the H-plane beamwidth at higher frequency.

Fig. 9 shows the E-plane measured maximum cross-polarization level at $\Theta = 0°$ and the simulated cross-polarization level at the angle of maximum beam direction. The E-plane cross-polarization level is nearly constant with frequency, but it increases by approximately 15 dB as the radius of curvature decreases. The highest cross-polarization level is at an angle approximately 30 degree off axis. The measured H-plane cross polarization level remains below 15 dB across the entire frequency band and below 20 dB over most of the band. The H-plane cross polarization does not have a preferential direction.

VI. Conclusion

Curving a DETSA around a foam cylinder in the longitudinal direction rotates the radiation pattern in the direction of curvature, and the pattern is pointed in a direction that is tangent to the antenna at a point approximately one-third of its length from the feed. The gain decreases by only 1 dB for large radii of curvature, but the E-plane cross polarization level increases by 15 dB for the same radius of curvature. Although not shown here, simulations prove that the conclusions in the letter are not effected by the pad used to mount the SMA launcher.

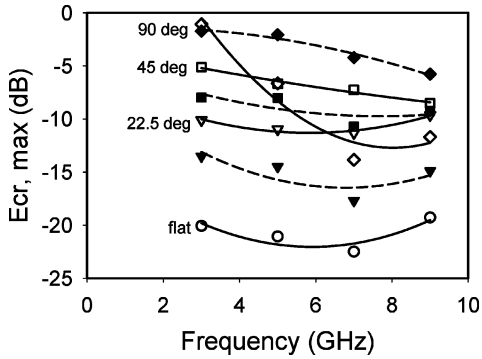

Fig. 9. Measured and simulated maximum E-plane cross polarization (open symbols are measured, solid symbols are simulated) (measured E-plane at $\theta = 0$, simulated E-plane at θ of maximum H copolarization).

References

[1] R. Q. Lee and R. N. Simons, "Tapered slot antenna," in *Advances in Microstrip and Printed Antennas*, K. F. Lee and W. Chen, Eds. New York: Wiley, 1997, pp. 443–514.

[2] L. R. Lewis, M. Fassett, and J. Hunt, "A broadband stripline array element," in *1974 IEEE AP-S Int. Symp. Dig.*, Atlanta, GA, Jun. 1974, pp. 335–337.

[3] P. J. Gibson, "The vivaldi aerial," in *9th Europ. Microw. Conf. Dig.*, Brighton, U.K., Sep. 1979, pp. 101–105.

[4] M. C. Greenberg, K. L. Virga, and C. L. Hammond, "Performance characteristics of the dual exponentially tapered slot antenna (DETSA) for wireless communications applications," *IEEE Trans. Veh. Technol.*, vol. 52, no. 2, pp. 305–312, Mar. 2003.

[5] K. S. Yngvesson, D. H. Schaubert, T. L. Korzeniowski, E. L. Kollberg, T. Thungren, and J. F. Johansson, "Endfire tapered slot antennas on dielectric substrates," *IEEE Trans. Antennas Propag.*, vol. AP-33, no. 12, pp. 1392–1400, Dec. 1985.

[6] R. Q. Lee and R. N. Simons, "Effect of curvature on tapered slot antennas," in *Proc. 1996 IEEE AP-S Antennas Propag. Int. Symp. Dig.*, Jul. 21–26, 1996, vol. 1, pp. 188–191.

[7] S. Nikolaou, L. Marcaccioli, G. E. Ponchak, J. Papapolymerou, and M. M. Tentzeris, "Conformal double exponentially slot antennas (DETSA) for UWB communications systems' front-ends," in *2005 IEEE Int. Conf. Ultra-Wideband (ICU 2005) Dig.*, Zurich, Switzerland, Sep. 5–8, 2005.

[8] D. C. Thompson, O. Tantot, H. Jallageas, G. E. Ponchak, M. M. Tentzeris, and J. Papapolymerou, "Characterization of liquid crystal polymer (LCP) material and transmission lines on LCP substrates from 30–110 GHz," *IEEE Trans. Microw. Theory Tech.*, vol. 52, no. 4, pp. 1343–1352, April 2004.

[9] J. B. Knorr, "Slot-line transitions," *IEEE Trans. Microw. Theory Tech.*, vol. 22, no. 5, pp. 548–554, May 1974.

[10] [Online]. Available: http://www.cst-america.com